Current-induced near-field radiative energy, linear-momentum, and angular-momentum transfer

Huimin Zhu,[1,4] Gaomin Tang [2,*] Lei Zhang [1,4,†] and Jun Chen[3,4,‡]

[1]*State Key Laboratory of Quantum Optics and Quantum Optics Devices, Institute of Laser Spectroscopy,*
Shanxi University, Taiyuan 030006, China
[2]*Graduate School of China Academy of Engineering Physics, Beijing 100193, China*
[3]*State Key Laboratory of Quantum Optics and Quantum Optics Devices, Institute of Theoretical Physics,*
Shanxi University, Taiyuan 030006, China
[4]*Collaborative Innovation Center of Extreme Optics, Shanxi University, Taiyuan 030006, China*

In this paper, we study the near-field radiative energy, linear-momentum, and angular-momentum transfer from a current-biased graphene to nanoparticles. The electric current through the graphene sheet induces nonequilibrium fluctuations, causing energy and momentum transfer even in the absence of a temperature difference. The inherent spin-momentum locking of graphene surface plasmons leads to an in-plane torque perpendicular to the direction of the electric current. In the presence of a temperature difference, the energy transfer is greatly enhanced while the lateral force and torque remain within the same order. Our work explores the potential of utilizing current-biased graphene to manipulate nanoparticles.

I. INTRODUCTION

The inclusion of nonreciprocal effects in the study of near-field thermal radiation has led to the discovery of various novel phenomena and has attracted significant scientific interest [1–9]. Nonreciprocity can be achieved in various scenarios. One example is by applying a magnetic field to magneto-optic materials [1–6]. Another approach is to use magnetic Weyl semimetals that have intrinsic time-reversal symmetry breaking [10–13].

Nonreciprocity-induced lateral force has been studied recently [14–17]. An atom or nanoparticle placed above a sample with mobile carrier drift experiences a fluctuation force [14]. In a system where vacuum-separated plates are at different temperatures, if at least one plate is nonreciprocal material, the setup can function as a heat engine where thermal energy is converted into mechanical work [15]. When a dipolar particle is placed in the vicinity of a nonreciprocal plasmonic slab, it experiences a lateral force and torque in the presence of a temperature difference between the particle and the slab [16]. The force is linked to the nonreciprocity of the surface polaritons and the torque to the spin-momentum locking of the surface polaritons.

Current-biased graphene is also known for its nonreciprocity [18–21]. The exceptional electron mobility of graphene allows it to sustain nonreciprocal surface plasmon polaritons (SPPs) when driven by an electric current, which gives rise to interesting properties such as Fizeau drag [22,23] and negative Landau damping [24]. Current-biased graphene is

in a nonequilibrium state and this leads to a finite photonic chemical potential [25] that depends on the in-plane wave vector for the thermal electromagnetic radiation. The occupation number of radiative photons is nonreciprocal, that is asymmetric with respect to the positive and negative in-plane wave vectors [26–29]. The nonreciprocal properties of current-biased graphene can be adjusted through chemical doping or gate voltage, making it suitable for a wide range of applications in controlling thermal radiation. For example, near-field radiative heat transfer has been studied between two suspended graphene sheets [30], graphene covered substrates [31], graphene-nanoparticles [32], and graphene-based multilayer systems [33]. However, the physical aspects of the force and torque experienced by the nanoparticle near the current-biased graphene remain unexplored to date.

In this paper, we investigate the near-field transfer of energy, linear momentum, and angular momentum between an isotropic dipolar nanoparticle and the current-biased graphene. The nonequilibrium state in the current-biased graphene induces energy transfer between the nanoparticle and the graphene even in the absence of a temperature difference. Importantly, these SPPs carry both a linear and spin-locked angular momentum. As a result, there is an exchange of net linear and spin angular momentum between the particle and the SPPs, leading to both lateral force and torque experienced by the nanoparticle.

II. SYSTEM AND FORMALISM

The system is illustrated schematically in Fig. 1(a), where the spherical nanoparticle with radius R is placed near the surface of current-biased monolayer graphene. Without losing generality, we assume that the drift velocity v_d in graphene is along the positive direction of the x axis. Within the

*gmtang@gscaep.ac.cn
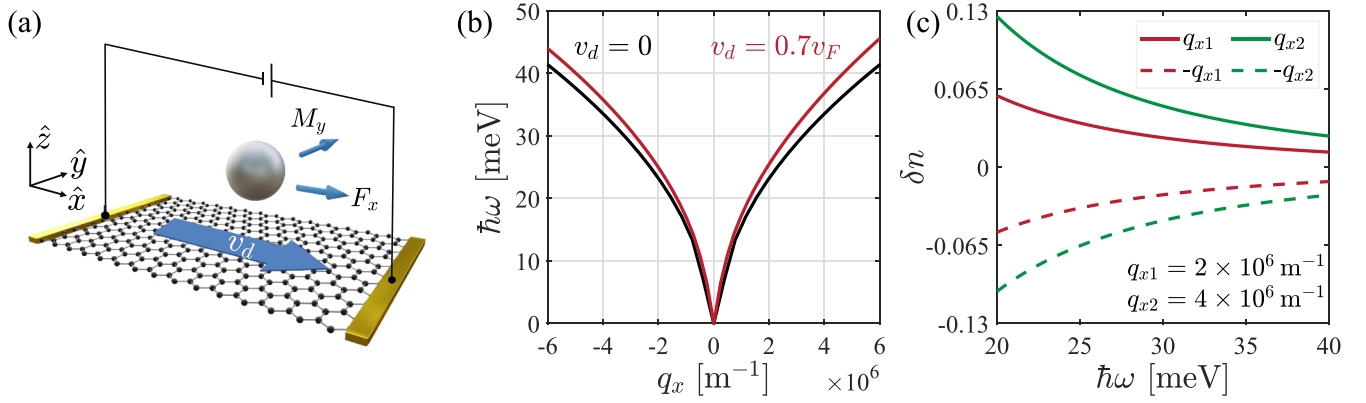†zhanglei@sxu.edu.cn
‡chenjun@sxu.edu.cn

FIG. 1. (a) Schematic plot of the lateral force and torque exerted on an isotropic dipolar particle above a current-biased graphene in the near-field regime. The drift velocity v_d is along the x direction. (b) Dispersion of the SPPs of the current-biased graphene. The electric current effectively drags the SPPs which leads to the property of nonreciprocal propagation. (c) The photon occupation number difference $\delta n(\omega, q_x)$ vs ω with $v_d = 0.7v_F$.

framework of fluctuational electrodynamics, the total power H, lateral force along the x direction F_x, and torque along the y direction M_y can be expressed as

$$P = \int_0^\infty \frac{d\omega}{2\pi} p(\omega), \qquad (1)$$

with $P \in \{H, F_x, M_y\}$ and the corresponding spectral densities $p \in \{h, f_x, m_y\}$. The spectral densities are given by [16]

$$h(\omega) = -\hbar\omega k_0^2 \, \text{Im}[\alpha(\omega)] \int \frac{d^2\boldsymbol{q}}{(2\pi)^2} \Theta(\omega, \boldsymbol{q}) \delta n(\omega, q_x), \quad (2)$$

$$f_x(\omega) = \hbar k_0^2 \, \text{Im}[\alpha(\omega)] \int \frac{d^2\boldsymbol{q}}{(2\pi)^2} q_x \Theta(\omega, \boldsymbol{q}) \delta n(\omega, q_x), \quad (3)$$

$$m_y(\omega) = -\hbar \, \text{Im}[\alpha(\omega)] \int \frac{d^2\boldsymbol{q}}{(2\pi)^2} q_x \text{Im}(r_p e^{2i\beta_0 d}) \delta n(\omega, q_x), \tag{4}$$

with

$$\Theta(\omega, \boldsymbol{q}) = \text{Re}\left[\frac{r_p e^{2i\beta_0 d}}{2\beta_0}\left(\frac{2q^2}{k_0^2} - 1\right)\right], \qquad (5)$$

where the Fresnel reflection coefficient for p polarization is given by

$$r_p = \frac{\beta_0 \sigma_g}{2\epsilon_0 \omega + \beta_0 \sigma_g}. \qquad (6)$$

Here, σ_g is the surface conductivity of graphene, and ϵ_0 is the dielectric constant in vacuum. The in-plane wave vector and the angular frequency are denoted by $\boldsymbol{q} = (q_x, q_y)$ and ω. The magnitude of the out-of-plane wave vector in air is $\beta_0 = \sqrt{k_0^2 - q^2}$ with $k_0 = \omega/c$ and $q = |\boldsymbol{q}|$. When an electric current is applied to the graphene so that the electrons near the Fermi surface experience a drift velocity, the system is not in local thermal equilibrium and the occupation number of the photons radiated from graphene is Doppler shifted. By assuming a drift velocity v_d in the x direction, the photon-occupation difference between the graphene and the nanoparticle is [8,26–29]

$$\delta n(\omega, q_x) = [e^{\hbar(\omega - q_x v_d)/k_B T_e} - 1]^{-1} - [e^{\hbar\omega/k_B T_p} - 1]^{-1}, \quad (7)$$

where T_e and T_p are the temperatures of graphene and the nanoparticle, respectively. In getting the occupation number of the photons radiated from the current-biased graphene, one needs to apply the condition that $\hbar q_x v_d$ is much smaller than the chemical potential [29]. Equation (7) indicates that the electric current-induced nonequilibrium fluctuations can produce a finite energy flux even in the absence of a temperature difference. In the following, we assume that the temperature of the particle and the graphene is the same with $T_p = T_e = T = 300$ K, unless there is a special account for the temperatures. The energy transmission function of the energy flux in Eq. (2) is defined through $h(\omega) = \int d^2\boldsymbol{q}\,\mathcal{Z}_h(\omega, \boldsymbol{q})/4\pi^2$ with

$$\mathcal{Z}_h(\omega, \boldsymbol{q}) = -\hbar\omega k_0^2 \, \text{Im}[\alpha(\omega)]\Theta(\omega, \boldsymbol{q})\delta n(\omega, q_x), \quad (8)$$

which provides the information of the energy transfer at given ω and $\boldsymbol{q}$. Similar definitions are, respectively, applied to the force and torque.

The dispersion relation of SPPs in a monolayer graphene can be obtained through [34]

$$2\epsilon_0 \omega + \beta_0 \sigma_g = 0, \qquad (9)$$

where the nonlocal surface conductivity σ_g is given by [35]

$$\sigma_g(\omega, q_x, q_y) = \frac{ie_0^2 \omega}{q^2} \frac{\mu(T)}{(\pi\hbar v_F)^2} \int_0^{2\pi} d\theta \frac{1}{(1 - \cos\theta v_d/v_F)^2}$$
$$\times \frac{q_x(\cos\theta - v_d/v_F) + q_y\sin\theta}{(\hbar\omega + i\gamma)/(\hbar v_F) - q_x\cos\theta - q_y\sin\theta}, \tag{10}$$

with $\mu(T) = 2k_B T \ln[2\cosh(\mu_g/2k_B T)]$. Here, T is the temperature, μ_g is the chemical potential, γ the damping parameter, and e_0 the electron charge. The nonlocal surface conductivity is obtained under the long-wavelength limit and by neglecting the interband transition which is justifiable for $2\mu_g > \hbar\omega$. In the numerical calculation, we set the Fermi velocity $v_F = 10^6$ m/s, the chemical potential $\mu_g = 0.1$ eV, and the damping parameter $\gamma = 3.7$ meV. Figure 1(b) shows the nonreciprocal dispersions of SPPs in the presence of an electric current.
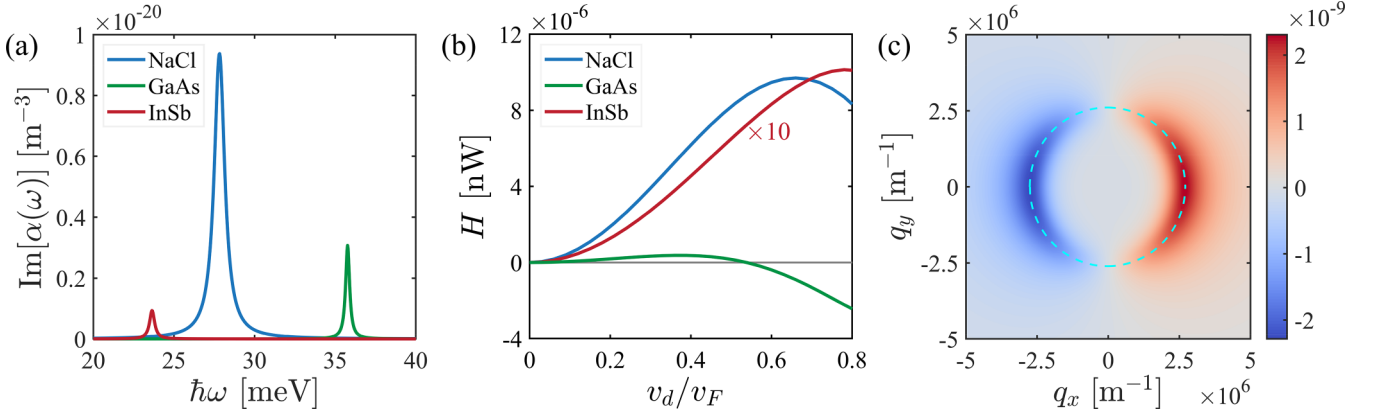
FIG. 2. (a) Imaginary part of the polarizability for different nanoparticles with radius $R = 40$ nm. (b) Net power transfer experienced by nanoparticles as a function of v_d at a separation distance of $d = 0.2$ μm. The curve for the InSb particle is multiplied by a factor of 10 for better visibility. (c) Energy transmission function $\mathcal{Z}_h$ (in units of nJ nm^2) plotted against q_x and q_y at $v_d = 0.3v_F$, $d = 0.2$ μm, and $\hbar\omega = 27.8$ meV. The cyan dashed line represents the dispersion of graphene SPPs.

III. NUMERICAL RESULTS

Before considering the nonequilibrium energy and momentum transfer, we discuss the nonreciprocal properties of $\delta n(\omega, q_x)$ shown in Fig. 1(c). We can see that the photon occupation number difference $\delta n(\omega, q_x)$ is positive for positive q_x under $\omega > q_x v_d$. This indicates that the effective photonic temperature of the graphene is higher than the particle temperature T_p. Furthermore, it should be noted that contributions from $\omega < q_x v_d$ can be disregarded. This is because these contributions become significant only when the separation between the particle and the graphene reaches subnanometer scales [28], whereas in our case, the distance is on the order of micrometers. Consequently, photons, especially those with positive q_x, flow from the graphene to the particle. In contrast, for negative q_x, $\delta n(\omega, q_x)$ is always negative. Therefore, the effective photonic temperature of the graphene is lower than T_p. This sign reversal indicates a reversal in the direction of photon transfer compared to the behavior exhibited by positive q_x.

We consider three kinds of nanoparticle: NaCl, undoped GaAs, and InSb. The intricate dielectric characteristics are given by the Lorentz-Drude model with

$$\varepsilon(\omega) = \varepsilon_\infty \frac{\omega_L^2 - \omega^2 - i\Gamma\omega}{\omega_T^2 - \omega^2 - i\Gamma\omega}, \tag{11}$$

where ε_∞ is the high-frequency dielectric constant, ω_L is the longitudinal optic-phonon frequency, ω_T is the transverse optic-phonon frequency, and Γ is the optic-phonon damping constant. Within the electrostatic limit, we can reasonably neglect multiple scattering interactions between the particle and the graphene, and describe the particle effectively using its electrical polarizability which is expressed as $\alpha(\omega) = 4\pi R^3[\varepsilon(\omega) - 1)]/[\varepsilon(\omega) + 2]$ [36]. It is important to note that these assumptions are valid only under the condition of $R \ll d \ll \hbar c/k_B T$. In Fig. 2(a), we present the imaginary part of the polarizability for these nanoparticles, revealing distinct dipolar resonances.

Now we study the effect of drift velocity on the net power transfer experienced by different nanoparticles, as shown in Fig. 2(b). We differentiate between positive and negative energy fluxes, which represent the flow of energy from the graphene to the particle and from the particle to the graphene, respectively. Our analysis reveals intriguing behaviors. For NaCl and InSb particles, the power transfer initially increases as v_d increases. However, with increasing v_d further, the power transfer decreases. In contrast, the direction of net power transfer undergoes a change for GaAs particles as the drift velocity increases. These are due to the interplay between the nonreciprocity of the SPPs and photon occupation number of graphene.

To analyze the contributions of forward ($q_x > 0$) and backward ($q_x < 0$) SPPs to net power transfer, we use the NaCl particle as an example. In Fig. 2(c), we show the energy transmission function and the dispersion of graphene plasmons (shown by the cyan dashed line). This visual representation aligns the bright branches of the energy transmission function with the cyan dashed line, confirming the dominant role played by SPPs in governing power transfer. For $q_x > 0$, the energy transfer coefficients are positive, indicating energy transfer from graphene to the particle. For $q_x < 0$, the energy transfer coefficients are negative, signifying energy transfer from the particle back to the graphene. The net energy transfer is the sum of contributions from $q_x > 0$ and $q_x < 0$. At lower drift velocities, the nonreciprocal characteristics of SPPs are not pronounced, and energy transfer is mainly governed by the nonreciprocal photon occupation number difference $\delta n(\omega, q_x)$, as shown in Fig. 1(c). However, as the drift velocity increases, nonreciprocal SPPs interplay with $\delta n(\omega, q_x)$. The high drift velocities suppress the net power transfer due to the nonreciprocal photon occupation number even change the energy transfer direction between GaAs and graphene.

In the following, we investigate the transfer of linear and angular momenta between the nanoparticles and the current-biased graphene. We define positive M_y along the negative y direction and positive F_x as oriented in the positive x direction. Our findings revealed a nonmonotonic behavior: Both force [Fig. 3(a)] and torque [Fig. 3(b)] increase with increasing the drift velocity up to a certain value, then start to decrease. This behavior is consistent with the energy transfer.
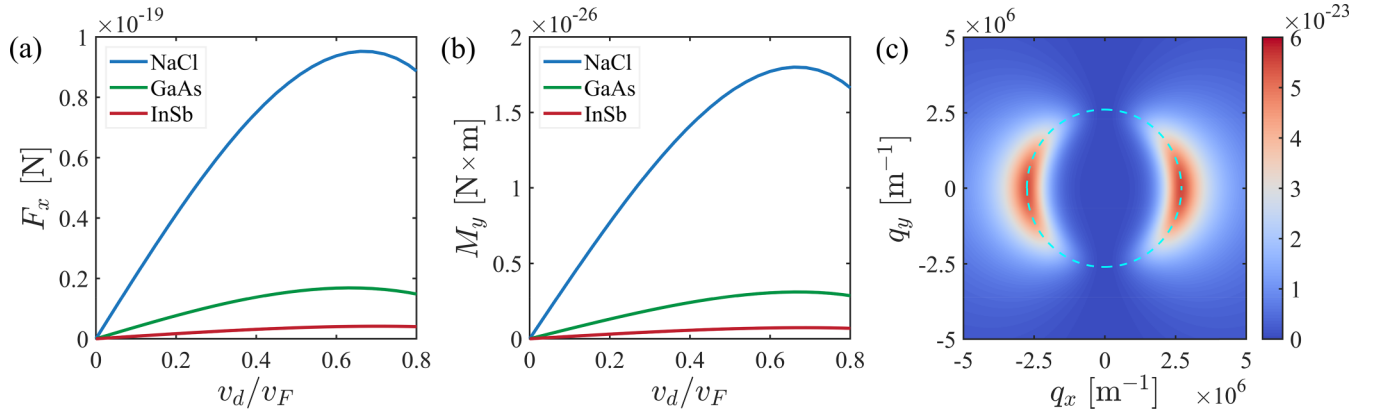
FIG. 3. (a) Net force on different nanoparticles as a function of v_d at $d = 0.2$ μm. (b) Net torque as a function of v_d at $d = 0.2$ μm. (c) Torque spectral density m_y (in units of nJ nm^2 s) as a function of q_x and q_y at $\hbar\omega = 27.8$ meV and $v_d = 0.3v_F$. The cyan dashed line represents the dispersion of graphene SPPs.

To have a deeper understanding of the force and torque acting on the particle, we analyze the exchange of linear momentum and spin angular momentum between the forward ($q_x > 0$) and backward ($q_x < 0$) SPPs and the nanoparticle. When photons transfer from the graphene to the particle ($q_x > 0$), the particle gains momentum, contributing to the lateral force along the positive x direction. Conversely, when $q_x < 0$, the particle loses momentum due to the reverse photon transfer, producing a lateral force in the same direction. Therefore, SPPs with both positive and negative q_x generate a net lateral force directed along the positive x direction. Due to the spin-momentum locking of SPPs [37], the transverse spin of SPPs strongly couples with their propagation direction. As a result, when SPPs propagate in the positive (negative) x direction, their spin aligns with the negative (positive) y direction, respectively. This spin angular-momentum transfer is facilitated by photon transfer from the graphene to the particle in the case of $q_x > 0$, generating a torque directed along the negative y direction. Importantly, the torque contributed from $q_x < 0$ is also along the negative y direction. Consequently, the net lateral torque is along the negative y direction. These are supported by Fig. 3(c) which shows the torque spectral density m_y as a function of q_x and q_y at $\hbar\omega = 27.8$ meV and $v_d = 0.3v_F$. Notably, for both positive and negative q_x, the torque spectral densities m_y are positive. Remarkably, the force and torque induced by current-biased graphene are of the same order of magnitude as those generated by thermally excited nonreciprocal surface electromagnetic waves [16].

Finally, we consider the scenario where the temperature of the particle differs from that of the graphene. Figures 4(a) and 4(b) show the dependence of net energy transfer and lateral force on the NaCl particle at various temperatures of the graphene. The nanoparticle temperature is at 300 K. Notably, the energy transfer from the graphene to the nanoparticle increases by three orders of magnitude. To explain this, we calculate the contributions from both the forward and backward SPPs at $T_e > T_p$ [see Figs. 4(c) and 4(d)]. It can be seen from Fig. 4(c) that the energy transfer for photons with opposite momentum has the same sign, which is completely different from the case in the absence of a temperature difference. This means that the contribution from the temperature difference dominates over that from the electric current.

Therefore, the energy transfer is greatly enhanced in the presence of a temperature difference. In contrast, the photons with $q_x > 0$ and $q_x < 0$ make positive and negative contributions to the force, respectively. We find that the force experienced by the particle does not differ significantly from that without a temperature difference. The torque has similar behavior as the force. Thus, the temperature difference has a marginal impact on the lateral force and torque while significantly enhancing the net power transfer with $T_e > T_p$.

IV. CONCLUSION

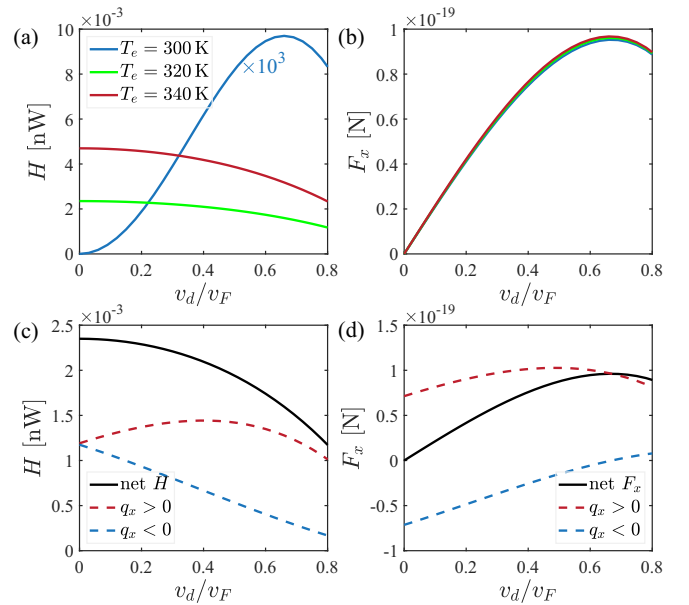We have investigated the near-field radiative energy, linear-momentum, and angular-momentum transfer from a

FIG. 4. (a) Net power and (b) net force for the NaCl particle as a function of v_d at various temperatures T_e in graphene with $T_p = 300$ K and $d = 0.2$ μm. The curve of power transfer at $T_e = 300$ K is multiplied by 10^3 for better visibility. (c) Net power and (d) net force vs v_d with $T_e = 320$ K and $T_p = 300$ K. The contributions from the forward ($q_x > 0$) and backward ($q_x < 0$) SPPs are separately shown.

current-biased graphene sheet to nanoparticles. Notably, for the GaAs particle, both the magnitude and the direction of energy transfer can be electrically manipulated. This unique phenomenon results from the interplay of nonreciprocal photon occupation differences and graphene surface plasmon polaritons. Moreover, in the presence of a temperature difference, our study reveals distinct energy transfer behavior while maintaining consistent force characteristics compared to the scenario without a temperature difference. Recently, measuring energy transfer, force, and torque between nanoparticles and surfaces has been experimentally realized [38–40], so our theoretical predictions can thus be realized in the near future.

APPENDIX: DERIVATION OF THE SPECTRAL DENSITIES OF THE POWER TRANSFER, THE FORCE, AND THE TORQUE

From the fluctuational electrodynamics, the spectral densities of the net power transfer from the particle to the environment h, the force f_j, and the torque m_j can be expressed as [41,42]

$$h(\omega) = \omega \, \mathrm{Im} \big[\langle p_j^{\mathrm{fl}*}(\omega) E_j^{\mathrm{ind}}(\omega) + p_j^{\mathrm{ind}*}(\omega) E_j^{\mathrm{fl}}(\omega) \rangle \big], \quad \text{(A1)}$$

$$f_j(\omega) = \mathrm{Re} \big[\langle p_k^{\mathrm{fl}}(\omega) \partial_j E_k^{\mathrm{ind}*}(\omega) + p_k^{\mathrm{ind}}(\omega) \partial_j E_k^{\mathrm{fl}*}(\omega) \rangle \big], \quad \text{(A2)}$$

$$m_j(\omega) = \epsilon_{jkl} \, \mathrm{Re} \big[\langle p_k^{\mathrm{fl}}(\omega) E_l^{\mathrm{ind}*}(\omega) + p_k^{\mathrm{ind}}(\omega) E_l^{\mathrm{fl}*}(\omega) \rangle \big], \quad \text{(A3)}$$

where the Einstein summation convention is applied with $j, k, l \in \{x, y, z\}$, and $\langle \cdots \rangle$ denotes the statistical ensemble average. E^{fl} is the electric field generated by current fluctu-

ations in the surface, p^{fl} is the dipole moment generated by the fluctuation of the particle dipole moment, E^{ind} is the field induced by the particle dipole moment fluctuations, and p^{ind} is the dipole moment induced in the particle by the environment field fluctuations. We assume that the nanoparticle is located at $\boldsymbol{r}$, and the dependence of $\boldsymbol{r}$ for the quantities on the right-hand sides are not written out explicitly.

The dipole moment induced by the electric-field fluctuations is given by

$$p_j^{\mathrm{ind}}(\boldsymbol{r}) = \epsilon_0 \alpha_{jk} E_k^{\mathrm{fl}}(\boldsymbol{r}), \quad \text{(A4)}$$

where α is the polarizability of the particle. The induced field by the dipole fluctuations can be expressed as

$$E_j^{\mathrm{ind}}(\mathbf{r}_2, \omega) = \omega^2 \mu_0 G_{jk}(\mathbf{r}_2, \mathbf{r}, \omega) p_k^{\mathrm{fl}}(\mathbf{r}, \omega), \quad \text{(A5)}$$

where the Green's function in the dipole-plate geometry is expressed as [43]

$$G(\mathbf{r}_2, \mathbf{r}_1, \omega) = \int \frac{d^2 \boldsymbol{q}}{(2\pi)^2} e^{i\boldsymbol{q}\cdot(\mathbf{R}_2 - \mathbf{R}_1)} G(\mathbf{q}, z_1 + z_2, \omega), \quad \text{(A6)}$$

with

$$G(\mathbf{q}, z_1 + z_2, \omega) = e^{i\beta_0(z_1 + z_2)} \frac{i r_p}{2\beta_0} \hat{\mathbf{e}}_{p+} \hat{\mathbf{e}}_{p-}^T. \quad \text{(A7)}$$

Here, we use the notation $\mathbf{r}_n = (\mathbf{R}_n, z_n)$ with $n = 1, 2$. The polarization vectors $\hat{\mathbf{e}}_{p\pm}^T$ for the p polarized mode along the $\pm z$ direction are

$$\hat{\mathbf{e}}_{p\pm}^T = \frac{1}{k_0}(\mp \beta_0 \cos\phi, \mp \beta_0 \sin\phi, q). \quad \text{(A8)}$$

The in-plane wave vector is $\boldsymbol{q} = (q_x, q_y) = q(\cos\phi, \sin\phi)$ where ϕ is the angle with respect to the x axis. The out-of-plane wave vector in air is $\beta_0 = \sqrt{k_0^2 - q^2}$ with $k_0 = \omega/c$. The Fresnel reflection coefficient for p polarization is denoted as r_p.

The correlations functions of the fluctuating quantities, p^{fl} and E^{fl}, respectively, satisfy the following fluctuation-dissipation relations with [44]

$$\langle p_j^{\mathrm{fl}}(\mathbf{r}, \omega) p_k^{\mathrm{fl}*}(\mathbf{r}, \omega') \rangle = (1/2i) \hbar \epsilon_0 [\alpha_{jk}(\omega) - \alpha_{kj}^*(\omega)]$$
$$\times \big[n(T_p, \omega) + \tfrac{1}{2} \big] 2\pi \delta(\omega - \omega'), \quad \text{(A9)}$$

and

$$\langle E_j^{\mathrm{fl}}(\mathbf{r}_1, \omega) E_k^{\mathrm{fl}*}(\mathbf{r}_2, \omega') \rangle = (1/2i) \int \frac{d^2 \boldsymbol{q}}{(2\pi)^2} [e^{i\boldsymbol{q}\cdot(\mathbf{R}_1 - \mathbf{R}_2)} G_{jk}(\mathbf{q}, z_1 + z_2, \omega) - e^{i\boldsymbol{q}\cdot(\mathbf{R}_2 - \mathbf{R}_1)} G_{kj}^*(\mathbf{q}, z_1 + z_2, \omega)](\hbar\mu_0\omega^2)$$

$$\times \left[n(T_e, \omega - q_x v_d) + \frac{1}{2} \right] 2\pi \delta(\omega - \omega') \delta(\mathbf{r}_2 - \mathbf{r}_1), \quad \text{(A10)}$$

where $n(T, \omega) = [\exp(\hbar\omega/k_B T) - 1]^{-1}$ is the Bose-Einstein distribution function at temperature T. Here, the correlation functions are antisymmetrized. The temperatures of the nanoparticle and the graphene are, respectively, denoted as T_p and T_e. The photon occupation number radiated from the graphene is Doppler shifted due to the electric current-induced drift velocity v_d in the x direction [8,26–29]. To get equal frequency correlations, the factor of 2π in front of the delta functions in the above correlation functions is canceled by integrating over frequency ω'.

The radiation power spectral density can be obtained as

$$
h(\omega) = \omega \operatorname{Im}\left[\omega^2 \mu_0 \langle p_j^{\mathrm{fl}*}(\mathbf{r}, \omega) p_k^{\mathrm{fl}}(\mathbf{r}, \omega)\rangle G_{jk}(\mathbf{r}, \mathbf{r}, \omega) + \epsilon_0 \alpha^*(\omega) \langle E_j^{\mathrm{fl}*}(\mathbf{r}, \omega) E_j^{\mathrm{fl}}(\mathbf{r}, \omega)\rangle\right]
$$

$$
= -\frac{\hbar \omega^3}{c^2} \operatorname{Im}[\alpha(\omega)] \int \frac{d^2\boldsymbol{q}}{(2\pi)^2} \operatorname{Im}[G_{jj}(\mathbf{q}, 2d, \omega)] \delta n(\omega, q_x), \tag{A11}
$$

with the photon-occupation difference

$$
\delta n(\omega, q_x) = \left[e^{\hbar(\omega - q_x v_d)/k_B T_e} - 1\right]^{-1} - \left[e^{\hbar\omega/k_B T_p} - 1\right]^{-1}. \tag{A12}
$$

We define the energy transmission function $\mathcal{Z}_h(\omega, \boldsymbol{q})$ through

$$
h(\omega) = \int \frac{d^2\boldsymbol{q}}{(2\pi)^2} \mathcal{Z}_h(\omega, \boldsymbol{q}), \tag{A13}
$$

so that

$$
\mathcal{Z}_h(\omega, \boldsymbol{q}) = -\hbar\omega k_0^2 \operatorname{Im}[\alpha(\omega)] \Theta(\omega, \boldsymbol{q}) \delta n(\omega, q_x), \tag{A14}
$$

with

$$
\Theta(\omega, \boldsymbol{q}) = \operatorname{Re}\left[r_p e^{2i\beta_0 d}\left(2q^2 - k_0^2\right)/\left(2\beta_0 k_0^2\right)\right]. \tag{A15}
$$

The spectral density of force can be obtained as

$$
f_x(\omega) = \operatorname{Re}\left[\langle p_k^{\mathrm{fl}}(\mathbf{r}, \omega) \partial_x\left(\omega^2 \mu_0 G_{kj}(\mathbf{r}, \mathbf{r}, \omega) p_j^{\mathrm{fl}}(\mathbf{r}, \omega)\right)^* + \epsilon_0 \alpha(\omega) E_k^{\mathrm{fl}}(\mathbf{r}, \omega) \partial_x E_k^{\mathrm{fl}*}(\mathbf{r}, \omega)\rangle\right]
$$

$$
= \hbar k_0^2 \operatorname{Im}[\alpha(\omega)] \int \frac{d^2\boldsymbol{q}}{(2\pi)^2} q_x \operatorname{Im}[G_{kk}(\mathbf{q}, 2d, \omega)] \delta n(\omega, q_x). \tag{A16}
$$

In the above, ∂_x represents the partial derivative in the x direction of position $\mathbf{r}$. The spectral density of torque can be obtained as

$$
m_y(\omega) = \omega^2 \mu_0 \operatorname{Re}\left[\langle p_z^{\mathrm{fl}}(\mathbf{r}, \omega) G_{xz}^*(\mathbf{r}, \mathbf{r}, \omega) p_z^{\mathrm{fl}*}(\mathbf{r}, \omega)\rangle - \langle p_x^{\mathrm{fl}}(\mathbf{r}, \omega) G_{zx}^*(\mathbf{r}, \mathbf{r}, \omega) P_x^{\mathrm{fl}*}(\mathbf{r}, \omega)\rangle\right]
$$

$$
+ \epsilon_0 \operatorname{Re}\left[\alpha(\omega) \langle E_z^{\mathrm{fl}}(\mathbf{r}, \omega) E_x^{\mathrm{fl}*}(\mathbf{r}, \omega)\rangle - \alpha(\omega) \langle E_x^{\mathrm{fl}}(\mathbf{r}, \omega) E_z^{\mathrm{fl}*}(\mathbf{r}, \omega)\rangle\right]
$$

$$
= \hbar k_0^2 \operatorname{Im}[\alpha(\omega)] \int \frac{d^2\boldsymbol{q}}{(2\pi)^2} \operatorname{Re}[G_{zx}(\mathbf{q}, 2d, \omega) - G_{xz}(\mathbf{q}, 2d, \omega)] \delta n(\omega, q_x). \tag{A17}
$$

We thus have

$$
f_x(\omega) = \int \frac{d^2\boldsymbol{q}}{(2\pi)^2} \mathcal{Z}_f(\omega, \boldsymbol{q}), \quad m_y(\omega) = \int \frac{d^2\boldsymbol{q}}{(2\pi)^2} \mathcal{Z}_m(\omega, \boldsymbol{q}), \tag{A18}
$$

with the force and the torque transmission functions, respectively, as

$$
\mathcal{Z}_f(\omega, \boldsymbol{q}) = \hbar k_0^2 q_x \operatorname{Im}[\alpha(\omega)] \Theta(\omega, \boldsymbol{q}) \delta n(\omega, q_x), \tag{A19}
$$

$$
\mathcal{Z}_m(\omega, \boldsymbol{q}) = -\hbar q_x \operatorname{Im}[\alpha(\omega)] \operatorname{Im}\left(r_p e^{2i\beta_0 d}\right) \delta n(\omega, q_x). \tag{A20}
$$

[1] E. Moncada-Villa, V. Fernández-Hurtado, F. J. García-Vidal, A. García-Martín, and J. C. Cuevas, Magnetic field control of near-field radiative heat transfer and the realization of highly tunable hyperbolic thermal emitters, Phys. Rev. B **92**, 125418 (2015).

[2] P. Ben-Abdallah, Photon thermal Hall effect, Phys. Rev. Lett. **116**, 084301 (2016).

[3] L. Zhu and S. Fan, Persistent directional current at equilibrium in nonreciprocal many-body near field electromagnetic heat transfer, Phys. Rev. Lett. **117**, 134303 (2016).

[4] I. Latella and P. Ben-Abdallah, Giant thermal magnetoresistance in plasmonic structures, Phys. Rev. Lett. **118**, 173902 (2017).

[5] R. M. Abraham Ekeroth, P. Ben-Abdallah, J. C. Cuevas, and A. García-Martín, Anisotropic thermal magnetoresistance for an active control of radiative heat transfer, ACS Photonics **5**, 705 (2018).

[6] A. Ott and S.-A. Biehs, Thermal rectification and spin-spin coupling of nonreciprocal localized and surface modes, Phys. Rev. B **101**, 155428 (2020).

[7] G. Tang, J. Chen, and L. Zhang, Twist-induced control of near-field heat radiation between magnetic Weyl semimetals, ACS Photonics **8**, 443 (2021).

[8] G. Tang, L. Zhang, Y. Zhang, J. Chen, and C. T. Chan, Near-field energy transfer between graphene and magneto-optic media, Phys. Rev. Lett. **127**, 247401 (2021).

[9] S.-A. Biehs, R. Messina, P. S. Venkataram, A. W. Rodriguez, J. C. Cuevas, and P. Ben-Abdallah, Near-field radiative heat transfer in many-body systems, Rev. Mod. Phys. **93**, 025009 (2021).

[10] B. Zhao, C. Guo, C. A. C. Garcia, P. Narang, and S. Fan, Axion-field-enabled nonreciprocal thermal radiation in Weyl semimetals, Nano Lett. **20**, 1923 (2020).

[11] C. Guo, B. Zhao, D. Huang, and S. Fan, Radiative thermal router based on tunable magnetic Weyl semimetals, ACS Photonics **7**, 3257 (2020).

[12] Y. Tsurimaki, X. Qian, S. Pajovic, F. Han, M. Li, and G. Chen, Large nonreciprocal absorption and emission of radiation in type-I Weyl semimetals with time reversal symmetry breaking, Phys. Rev. B **101**, 165426 (2020).

[13] S. Pajovic, Y. Tsurimaki, X. Qian, and G. Chen, Intrinsic nonreciprocal reflection and violation of Kirchhoff's law of radiation in planar type-I magnetic Weyl semimetal surfaces, Phys. Rev. B **102**, 165417 (2020).

[14] B. Shapiro, Fluctuation-induced forces in the presence of mobile carrier drift, Phys. Rev. B **96**, 075407 (2017).

[15] D. Gelbwaser-Klimovsky, N. Graham, M. Kardar, and M. Krüger, Near field propulsion forces from nonreciprocal media, Phys. Rev. Lett. **126**, 170401 (2021).

[16] C. Khandekar, S. Buddhiraju, P. R. Wilkinson, J. K. Gimzewski, A. W. Rodriguez, C. Chase, and S. Fan, Nonequilibrium lateral force and torque by thermally excited nonreciprocal surface electromagnetic waves, Phys. Rev. B **104**, 245433 (2021).

[17] Y. Tsurimaki, R. Yu, and S. Fan, Moving media as photonic heat engine and pump, Phys. Rev. B **107**, 115406 (2023).

[18] D. S. Borgnia, T. V. Phan, and L. S. Levitov, Quasi-relativistic Doppler effect and non-reciprocal plasmons in graphene, arXiv:1512.09044.

[19] B. V. Duppen, A. Tomadin, A. N. Grigorenko, and M. Polini, Current-induced birefringent absorption and non-reciprocal plasmons in graphene, 2D Mater. **3**, 015011 (2016).

[20] T. A. Morgado and M. G. Silveirinha, Drift-induced unidirectional graphene plasmons, ACS Photonics **5**, 4253 (2018).

[21] T. A. Morgado and M. G. Silveirinha, Nonlocal effects and enhanced nonreciprocity in current-driven graphene systems, Phys. Rev. B **102**, 075102 (2020).

[22] Y. Dong, L. Xiong, I. Y. Phinney, Z. Sun, R. Jing, A. S. McLeod, S. Zhang, S. Liu, F. L. Ruta, H. Gao, Z. Dong, R. Pan, J. H. Edgar, P. Jarillo-Herrero, L. S. Levitov, A. J. Millis, M. M. Fogler, D. A. Bandurin, and D. N. Basov, Fizeau drag in graphene plasmonics, Nature (London) **594**, 513 (2021).

[23] W. Zhao, S. Zhao, H. Li, S. Wang, S. Wang, M. I. B. Utama, S. Kahn, Y. Jiang, X. Xiao, S. Yoo, K. Watanabe, T. Taniguchi, A. Zettl, and F. Wang, Efficient Fizeau drag from Dirac electrons in monolayer graphene, Nature (London) **594**, 517 (2021).

[24] T. A. Morgado and M. G. Silveirinha, Negative Landau damping in bilayer graphene, Phys. Rev. Lett. **119**, 133901 (2017).

[25] C. H. Henry and R. F. Kazarinov, Quantum noise in photonics, Rev. Mod. Phys. **68**, 801 (1996).

[26] A. I. Volokitin and B. N. J. Persson, Theory of the interaction forces and the radiative heat transfer between moving bodies, Phys. Rev. B **78**, 155437 (2008).

[27] A. I. Volokitin and B. N. J. Persson, Quantum friction, Phys. Rev. Lett. **106**, 094502 (2011).

[28] A. I. Volokitin and B. N. J. Persson, Near-field radiative heat transfer between closely spaced graphene and amorphous SiO_2, Phys. Rev. B **83**, 241407(R) (2011).

[29] J. Peng and J.-S. Wang, Current-induced heat transfer in double-layer graphene, arXiv:1805.09493.

[30] Y. Zhang, C.-L. Zhou, L. Qu, and H.-L. Yi, Active control of near-field radiative heat transfer through nonreciprocal graphene surface plasmons, Appl. Phys. Lett. **116**, 151101 (2020).

[31] K. Shi, Z. Chen, Y. Xing, J. Yang, X. Xu, J. S. Evans, and S. He, Near-field radiative heat transfer modulation with an ultrahigh dynamic range through mode mismatching, Nano Lett. **22**, 7753 (2022).

[32] Y. Zhang, C.-L. Zhou, H.-L. Yi, and H.-P. Tan, Radiative thermal diode mediated by nonreciprocal graphene plasmon waveguides, Phys. Rev. Appl. **13**, 034021 (2020).

[33] C.-L. Zhou, L. Qu, Y. Zhang, and H.-L. Yi, Enhancement and active mediation of near-field radiative heat transfer through multiple nonreciprocal graphene surface plasmons, Phys. Rev. B **102**, 245421 (2020).

[34] P. A. D. Gonçalves and N. M. R. Peres, *An Introduction to Graphene Plasmonics* (World Scientific, Singapore, 2016).

[35] D. Svintsov and V. Ryzhii, Comment on "Negative Landau damping in bilayer graphene", Phys. Rev. Lett. **123**, 219401 (2019).

[36] R. Zhao, A. Manjavacas, F. J. G. de Abajo, and J. B. Pendry, Rotational quantum friction, Phys. Rev. Lett. **109**, 123604 (2012).

[37] K. Y. Bliokh, D. Smirnova, and F. Nori, Quantum spin Hall effect of light, Science **348**, 1448 (2015).

[38] F. Menges, M. Dittberner, L. Novotny, D. Passarello, S. S. P. Parkin, M. Spieser, H. Riel, and B. Gotsmann, Thermal radiative near field transport between vanadium dioxide and silicon oxide across the metal insulator transition, Appl. Phys. Lett. **108**, 171904 (2016).

[39] P. Ju, Y. Jin, K. Shen, Y. Duan, Z. Xu, X. Gao, X. Ni, and T. Li, Near-field GHz rotation and sensing with an optically levitated nanodumbbell, Nano Lett. **23**, 10157 (2023).

[40] J. Ahn, Z. Xu, J. Bang, P. Ju, X. Gao, and T. Li, Ultrasensitive torque detection with an optically levitated nanorotor, Nat. Nanotechnol. **15**, 89 (2020).

[41] C. Henkel, K. Joulain, J.-P. Mulet, and J.-J. Greffet, Radiation forces on small particles in thermal near fields, J. Opt. A: Pure Appl. Opt. **4**, S109 (2002).

[42] A. Manjavacas, F. J. Rodríguez-Fortuño, F. J. G. de Abajo, and A. V. Zayats, Lateral Casimir force on a rotating particle near a planar surface, Phys. Rev. Lett. **118**, 133605 (2017).

[43] C. Khandekar and Z. Jacob, Thermal spin photonics in the near-field of nonreciprocal media, New J. Phys. **21**, 103030 (2019).

[44] L. D. Landau and E. M. Lifshitz, *Course of Theoretical Physics: Statistical Physics Part 1* (Elsevier, Amsterdam, 2013), Vol. 5.